

# Observational limits on inverse Compton processes in gamma-ray bursts

Tsvi Piran,<sup>1</sup>★ Re'em Sari<sup>1,2</sup>★ and Yuan-Chuan Zou<sup>1</sup>★

<sup>1</sup>*Racah Institute for Physics, The Hebrew University, Jerusalem, 91904, Israel*

<sup>2</sup>*Theoretical Astrophysics, Caltech, Pasadena, CA 91125, USA*

Accepted 2008 November 2. Received 2008 November 2; in original form 2008 September 21

## ABSTRACT

Inverse Compton (IC) scattering is one of two viable mechanisms that can produce prompt non-thermal soft gamma-ray emission in gamma-ray bursts. IC requires low-energy seed photons and a population of relativistic electrons that upscatter them. The same electrons will upscatter the gamma-ray photons to even higher energies in the TeV range. Using the current upper limits on the prompt optical emission, we show that under general conservative assumption the IC mechanism suffers from an ‘energy crisis’. Namely, IC will overproduce a very high energy component that would carry much more energy than the observed prompt gamma-rays, or alternatively it will require a low-energy seed that is more energetic than the prompt gamma-rays. Our analysis is general, and it makes no assumptions on the specific mechanism that produces the relativistic electron population.

**Key words:** radiation mechanisms: non-thermal – ISM: jets and outflows – gamma-rays: bursts.

## 1 INTRODUCTION

The mechanism that produces the prompt gamma-ray emission in gamma-ray burst (GRBs) is still uncertain. The non-thermal character of the spectrum points towards Inverse Compton (IC) and synchrotron as the two natural candidates. The latter became, somehow, the ‘standard’ process, but the former always remained a serious alternative (Shemi 1994; Shaviv & Dar 1995; Sari, Narayan & Piran 1996; Sari & Piran 1997; Waxman 1997; Ghisellini et al. 2000; Stern & Poutanen 2004; Kobayashi et al. 2007 and others). The observations of numerous bursts with low-energy spectral slopes that are inconsistent with synchrotron (Cohen et al. 1997; Preece et al. 1998; Ghisellini et al. 2000; Preece et al. 2002) provided additional motivation to consider IC. Recently, Kumar & McMahon (2008) have shown further inconsistency with the overall synchrotron model and suggested that synchrotron self-Compton (SSC) can resolve some of these problems.

The recent observations of a naked eye optical flash from GRB 080319b (Bloom et al. 2008; D’Elia et al. 2008; Racusin et al. 2008) that coincided in time with the prompt gamma-ray emission provided further motivation to consider IC as the source of the prompt gamma-rays. Among the different models that appeared so far (Fan & Piran 2008; Kumar & Panaitescu 2008; Yu, Wang & Dai 2008; Zou, Piran & Sari 2008), several favour models in which the prompt gamma-ray emission is IC of the optical flash, and there have been suggestions that this is generic to many GRBs.

Motivated by these ideas, we examine here the possibility that IC is the source of the prompt soft gamma-ray emission in GRBs. This requires a soft component at the infrared (IR)–UV range that serves as the seed for the IC process. The flux of these seed photons is constrained by observations (or upper limits) of the prompt optical emission. GRB 990123 (Akerlof et al. 1999) and GRB 080319B (Racusin et al. 2008) are rare exceptions with very strong optical emission,  $\sim 9$  and  $\sim 5.3$  mag, respectively. However, most bursts are much dimmer optically with observations or upper limits around 14 mag (Yost et al. 2007). This should be compared with fluxes of mJy in soft gamma-rays for a modest burst. What is important, in this work, is the flux ratio  $F_\gamma/F_{\text{opt}}$  which is typically larger than 0.1 during the peak soft gamma-ray emission (Yost et al. 2007).

The basic problem of the IC model can be explained simply. If the low-energy seed emission is in the optical, while the observed soft gamma-ray spectrum is the first IC component, then second IC scatterings would create a TeV component. Upper limits or observations of the prompt optical signal show that the  $Y$  parameter, i.e. the ratio between the energy in the first IC component and that in the low-energy seed photons is very large, typically greater than thousands. Theory would then show that the second IC component in the TeV range would carry an even larger amount of energy, again by a factor of  $Y \gg 1$ , producing an ‘energy crisis’ for this model, and possibly violating upper limits from EGRET<sup>1</sup> (Gonzalez & Sanchez 2005; Ando, Nakar & Sari 2008). This problem is generic, and it does not depend on the specific details of the overall model.

★E-mail: tsvi@phys.huji.ac.il (TP); sari@tapir.caltech.edu (RS); zou@phys.huji.ac.il (YCZ)

<sup>1</sup> Energetic Gamma-Ray Experiment Telescope. Deeper upper limits on a wider energy range may soon come from Fermi, making our argument stronger.

The above analysis is oversimplified, and two factors may alleviate the energy catastrophe. First, the frequency of the seed photons may differ from that where upper limits exist, allowing larger seed flux and reducing the lower limits on  $Y$ . Secondly, the Klein–Nishina (KN) suppression, which does not affect the first scattering, may affect the second, resulting in a lower  $Y$  parameter for the second scattering than the first one. In this paper, we explore the parameter space to see whether there exists a regime where a combination of these two factors allows for less energy in the second IC component (typically in the TeV range) than in the gamma-rays. We find that possible solutions are limited to a very small region in the parameter space in which the seed photons are in the IR, the bulk Lorentz factor is very low ( $\leq 200$ ) and the electrons' Lorentz factor is very large ( $\geq 2000$ ). However, this solution implies a healthy emission in the IR, while self-absorption limits it. Therefore, when taking self-absorption into account, this solution is ruled out as well. A second possible solution exists if the seed photons are in the UV. This solution requires a very low electron Lorentz factor ( $\leq 100$ ), and a seed photon flux that carries comparable energy to the observed prompt gamma-rays. Furthermore, prompt X-ray observations limit the high-energy tail of the UV component and practically rule out this model.

We take the Lorentz factor of the electrons and the bulk Lorentz factor as free parameters, and estimate the second IC fluence (at TeV or multi-GeV) given the observed prompt gamma-ray flux and the limits on the prompt optical band. Most of our analysis is insensitive to the size of the source, which appears only in the final section when we estimate the self-absorption flux. In our numerical examples, we use very conservative parameters. For example, we use an  $R$  magnitude of 11.2 as an upper limit on the optical flux, while many limits are much stronger and the gamma-ray flux we take,  $10^{-26}$  erg cm $^{-2}$  s $^{-1}$  Hz $^{-1}$ , is quite modest. Similarly, we use conservative rather than 'canonical' values for the spectral slopes.

## 2 BASIC EQUATIONS

Consider electrons that move with a bulk Lorentz factor  $\Gamma \gg 1$ , while in the bulk (or fluid) rest frame they have a typical Lorentz factor  $\gamma_e \gg 1$  in a random direction. We examine IC scattering of seed photons with a peak frequency  $\nu_{\text{seed}}$  and a peak flux  $F_{\text{seed}}$  (both measured at the observer's rest frame). We assume that the seed photons are roughly isotropic in the fluid's frame. This would be the case if the seed photons are produced by synchrotron radiation in the bulk, or any other mechanism local to the moving fluid. We will consider external IC, in which the seed photons are produced by an external source elsewhere. For simplicity, we assume that all the photons have the same energy and all the electrons have the same Lorentz factor. The energy and flux of the scattered photons are

$$\nu_{\text{IC}} = \nu_{\text{seed}} \gamma_e^2 \min(1, \xi^{-1}) \quad (1)$$

and

$$\nu_{\text{IC}} F_{\text{IC}} = \nu_{\text{seed}} F_{\text{seed}} Y \min(1, \xi^{-2}), \quad (2)$$

where  $Y \equiv \tau \gamma_e^2$  and  $\tau$  are the Compton parameter and the optical depth in the Thomson scattering regime. Note that the unknown optical depth,  $\tau$ , is introduced here in the definition of  $Y$ , but it is not used elsewhere in the paper. Our analysis is independent of this unknown factor. The factor,  $\xi$ , corresponds to the correction that arises if the scattering is in the KN region:

$$\xi \equiv \frac{(\gamma_e/\Gamma) h \nu_{\text{seed}}}{m_e c^2} > 1. \quad (3)$$

The expression given in equation (3) is approximate. Again, this approximation is sufficient for our purpose.

We now consider the possibility that the prompt gamma-rays arise due to IC scattering of a lower energy component. We now use the observed gamma-ray flux,  $F_\gamma$ , and its peak energy,  $\nu_\gamma$ , and the upper limits (or detections) of prompt optical emission,  $F_{\text{opt}}$ , at  $\nu_{\text{opt}}$  to set limits on the IC process.

The peak flux of the low-energy component,  $F_L$ , is at  $\nu_L$ , which is not necessarily at the observed frequency  $\nu_{\text{opt}}$ . Given an upper limit on the prompt optical flux,  $F_{\text{opt}}$ , at  $\nu_{\text{opt}}$  (or on the flux at any other frequency), we can set a limit on  $F_L$  if the optical frequency is in the same spectral region as  $\nu_L$ , the peak frequency of the lower spectral component of slope  $\alpha$ :

$$F_L \leq (\nu_L/\nu_{\text{opt}})^\alpha F_{\text{opt}}. \quad (4)$$

The equality here and elsewhere holds when  $F_{\text{opt}}$  corresponds to a detection and an inequality corresponds to an upper limit. There are two possibilities, either  $\nu_L > \nu_{\text{opt}}$ , which we call the 'UV solution', or  $\nu_L < \nu_{\text{opt}}$ , which we call the 'IR solution'. Since by definition the seed photon energy peaks at  $\nu_L$ , we must have  $\alpha > -1$  in the UV solution and  $\alpha < -1$  in the IR solution. Moreover, since the spectrum around  $\nu_L$  is upscattered to create the familiar band spectrum (Band et al. 1993) around  $\nu_\gamma$ , we can expect  $\alpha \approx -1.25$  for the IR solution and  $\alpha \approx 0$  for the UV solution.

As the first IC scattering results in soft gamma-rays, it is clearly away from the KN regime, and we obtain, using equations (1), (2) and (4), a limit on the Compton parameter  $Y_L$  in the first Compton scattering:

$$Y_L \geq \left( \frac{\nu_\gamma F_\gamma}{\nu_{\text{opt}} F_{\text{opt}}} \right) \left( \frac{\nu_L}{\nu_{\text{opt}}} \right)^{-(1+\alpha)}. \quad (5)$$

Using this limit, we turn now to the second-order IC component. This process will produce photons in the GeV–TeV range. As the scattered photon is energetic, it might be in the KN regime, and we have

$$\nu_{\text{H}} = \nu_\gamma \left( \frac{\nu_\gamma}{\nu_{\text{opt}}} \right) \left( \frac{\nu_{\text{opt}}}{\nu_L} \right) \min(1, \xi^{-1}) \quad (6)$$

and

$$Y_{\text{H}} \geq \left( \frac{\nu_\gamma F_\gamma}{\nu_{\text{opt}} F_{\text{opt}}} \right) \left( \frac{\nu_L}{\nu_{\text{opt}}} \right)^{-(1+\alpha)} \min(1, \xi^{-2}). \quad (7)$$

$Y_{\text{H}}$  is the ratio of energy emitted in the high-energy (TeV) band and in lower energy gamma-rays (see Fig. 1).

As a conservative numerical example, we will use the following typical parameters:  $F_\gamma = 10^{-26}$  erg cm $^{-2}$  s $^{-1}$  Hz $^{-1}$  and  $F_{\text{opt}} \leq 10^{-24}$  erg cm $^{-2}$  s $^{-1}$  Hz $^{-1}$ , leading to a ratio of  $F_\gamma/F_{\text{opt}} \geq 0.01$ . This optical flux corresponds to an  $R$  magnitude of 11.2, which is a very conservative upper limit to the prompt optical emission of most GRBs while the prompt gamma-ray flux is moderate. We use  $\nu_{\text{opt}} = 8 \times 10^{14}$  Hz and  $h\nu_\gamma = 500$  keV [both energies are larger by a factor of  $(1+z) \approx 2$  than the observed frequencies,  $R$  band and 250 keV]. Thus,  $\nu_\gamma F_\gamma / (\nu_{\text{opt}} F_{\text{opt}}) \geq 1500$ . We will use  $\Gamma = 300$  and  $\gamma_e \equiv (\nu_\gamma/\nu_{\text{opt}})^{1/2} \simeq 400$  for the canonical values of  $\nu_\gamma$  and  $\nu_{\text{opt}}$ . We find

$$h\nu_{\text{H}} = 0.08 \text{ TeV} \left( \frac{h\nu_\gamma}{500 \text{ keV}} \right) \left( \frac{\gamma_e}{400} \right)^2 \min \left[ 1, \frac{\Gamma m_e c^2}{\gamma_e h\nu_\gamma} \right] \quad (8)$$

and

$$Y_{\text{H}} \geq 1500 \left( \frac{F_\gamma}{10^{-26}} \frac{10^{-24}}{F_{\text{opt}}} \right) \left( \frac{h\nu_\gamma}{500 \text{ keV}} \frac{8 \times 10^{14} \text{ Hz}}{\nu_{\text{opt}}} \right) \times \left( \frac{\nu_L}{\nu_{\text{opt}}} \right)^{-(1+\alpha)} \min \left[ 1, \left( \frac{\Gamma m_e c^2}{\gamma_e h\nu_\gamma} \right)^2 \right]. \quad (9)$$

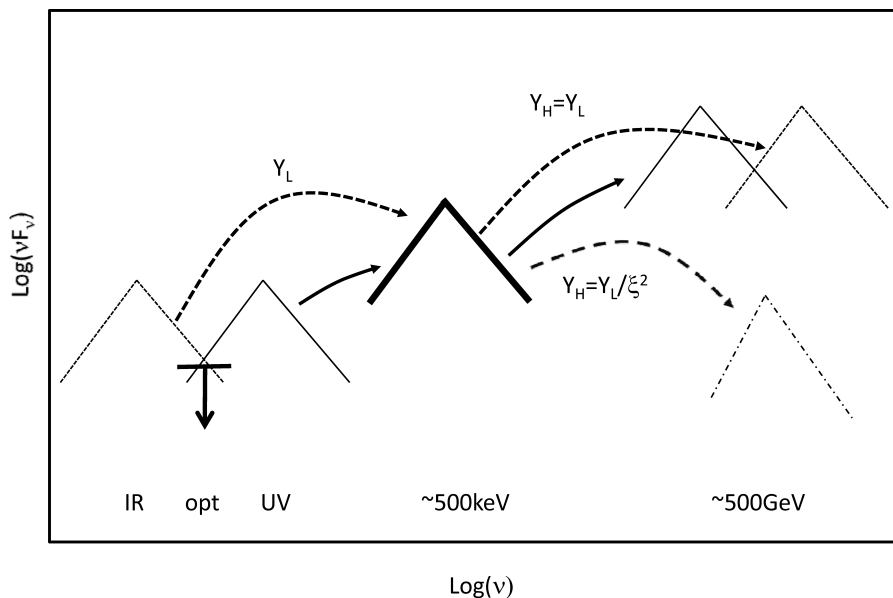


**Figure 1.** A schematic description of the IC process. Low-energy photons in the IR (marked in dotted lines), optical or UV (marked in solid thin lines) are IC scattered to produce the observed soft gamma-ray emission (marked in bold lines). A second IC scattering brings the soft gamma photons to the TeV region. If the initial seed photons are softer, the higher energy component is harder. If the initial seed is in the IR, then the second IC process might be in the KN regime, in which case this component is suppressed (dash-dotted line). The seed low-energy emission is constrained by upper limits on the optical prompt observations (bold solid arrow).

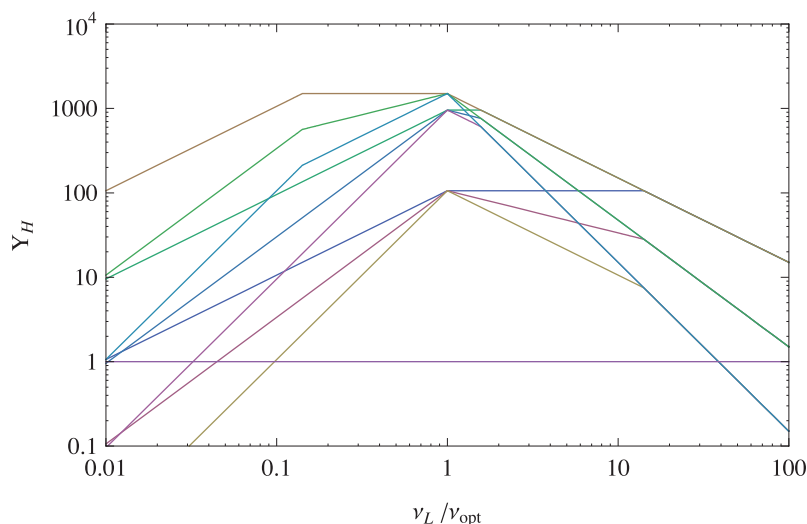


**Figure 2.**  $Y_H$  as a function of  $\nu_L/\nu_{\text{opt}}$  for  $\Gamma = 1000, 300, 100$  (from top to bottom) and  $\alpha = 0, 0.5, 1$  (from top to bottom) for  $\nu_L > \nu_{\text{opt}}$  and  $\alpha = -1, -1.5, -2$  for  $\nu_L < \nu_{\text{opt}}$ . The parameters used in this figure are as follows:  $F_\gamma/F_{\text{opt}} = 0.01$ ,  $\nu_{\text{opt}} = 8 \times 10^{14}$  Hz and  $h\nu_\gamma = 500$  keV. The breaks in the lines appear at  $\nu_L = \nu_{\text{opt}}$  when we change from negative to positive  $\alpha$  and at the frequency, which depends on  $\Gamma$ , where the KN correction begins.

The essence of the IC problem is the very large value of  $Y_H$ , which arises from the fact that the energy released in prompt gamma-rays is at least a factor of 1500 larger than the energy released in prompt optical emission (see equation 5). The large values of  $Y_H$  imply that the energy emitted in the TeV range exceeds the observed soft gamma-rays by several orders of magnitude.

Fig. 2 depicts  $Y_H$  as a function of  $\nu_L$  for different values of  $\Gamma$  and for different spectral indices.  $Y_H$  peaks when  $\nu_L = \nu_{\text{opt}}$ . This is expected, as in this case the observed limits on the lower energy flux are strongest. If  $\nu_L$  increases or decreases, more energy can be ‘hidden’ in the lower energy component and the corresponding  $Y_L$

and  $Y_H$  will be smaller. Because of a similar reason,  $Y_H$  decreases when  $|\alpha + 1|$  increases.

We find two possible regimes for IC solutions that are not overproducing a high-energy (TeV) component. The UV solution requires  $\nu_L > 10\nu_{\text{opt}}$  and  $\alpha \geq 1$ . The electrons’ Lorentz factor in the UV solution satisfies  $\gamma_e < 100$ . The second Compton scattering is not in the KN regime since  $\Gamma > 100$ , and correspondingly  $\xi$  is small. Since KN suppression is negligible  $Y_L \approx Y_H$  and the total energy, given by  $(1/Y_L + 1 + Y_H) E_\gamma$ , is at least  $3 E_\gamma$ . UV solutions with  $Y_L = Y_H < 1$  are therefore also wasteful as they require a large  $(E_\gamma/Y_L)$  low-energy component. A second problem arises, for this

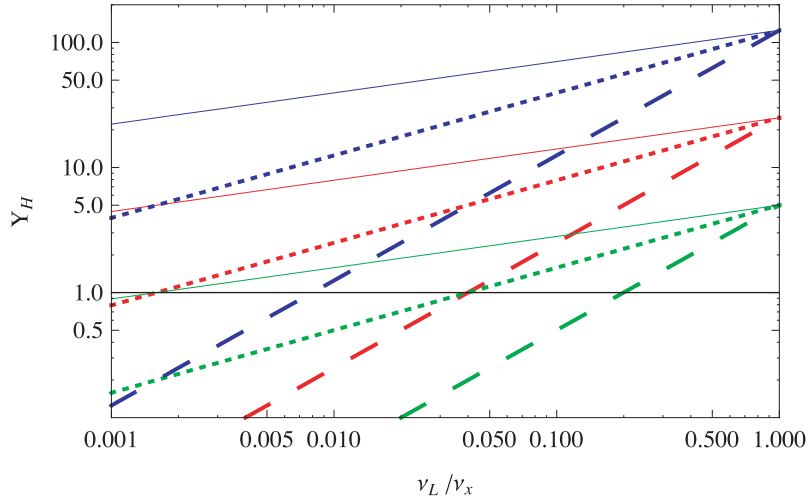


**Figure 3.**  $Y_H$  as a function of  $\nu_L/\nu_x$  for  $\alpha_1 = -0.5, 0, 0.5$  (blue, red and green) and  $\alpha_2 = -1.25, -1.5, -2$  (solid, dotted and dashed) for  $h\nu_x = 20$  keV and  $h\nu_\gamma = 500$  keV. The corresponding  $\gamma_e$  range is from 158 at  $\nu_L = 0.001\nu_x$  to 5 at  $\nu_L = \nu_x$ .

solution, with the spectral shape. The observed low-energy spectral index (in the X-ray band) is typically close to zero, while this solution requires a steeply rising flux from  $\nu_{\text{opt}}$  to  $\nu_L$ . Note that in Fig. 2 we show conservatively curves for  $\alpha = 0, 0.5, 1$  even though the ‘canonical’ value is 0. Moreover, unless there is a pair loading (i.e. if there is one electron per proton), then the low  $\gamma_e$  required for the UV solution implies that the protons carry significantly more energy than the electrons by at least a factor of  $m_p/\gamma_e m_e$ . Thus this solution is very inefficient.

The above analysis is based on the optical limits, but for the modest values of  $\gamma_e$  needed for the UV solution,  $\nu_L$ , the peak flux frequency of the seed photons becomes large (equation 1) and  $F_L$  is now limited by prompt soft X-ray observations in addition to the optical limits. For the discussion below, we use  $\alpha_1$  and  $\alpha_2$  as the low- and high-energy spectral indices, respectively. As already stated, the canonical values are  $\alpha_1 = 0$  and  $\alpha_2 = -1.25$  (Band et al. 1993).<sup>2</sup> One can estimate the X-ray flux at  $\nu_x = 20$  keV directly from the observations at this energy or using the flux at  $\nu_\gamma \approx 500$  keV and the low-energy spectral slope  $\alpha_1$ . Recalling that the IC does not change the spectral slope, we use the same indices both around  $\nu_\gamma$  and around  $\nu_L$ . Therefore,

$$F_L < (\nu_L/\nu_x)^{\alpha_2} (\nu_x/\nu_\gamma)^{\alpha_1} F_\gamma. \quad (10)$$

Using equation (2), we obtain

$$Y > \frac{\nu_\gamma^{\alpha_1+1} \nu_x^{\alpha_2-\alpha_1}}{\nu_L^{\alpha_2+1}} = (\nu_\gamma/\nu_x)^{\alpha_1-\alpha_2} \gamma_e^{2(\alpha_2+1)}. \quad (11)$$

Since the UV solution is not in the KN regime, we have  $Y = Y_L = Y_H$ . If we take the typical spectral indices below and above  $\nu_\gamma$  to be  $\alpha_1 = 0$  and  $\alpha_2 = -1.25$ , respectively (Band et al. 1993), and impose the condition  $Y \cong 1$  (where the total energy required is minimized to  $3E_\gamma$ ), we find that  $\gamma_e > 3000$  or  $\nu_L < \nu_{\text{opt}}$  – thus the whole UV regime is ruled out. This condition depends strongly on the spectral indices:  $\alpha_1$  and  $\alpha_2$ . Clearly, if  $\alpha_2$  is smaller (a steeper drop on the high-energy side)  $\nu_L$  can be larger and  $Y$  is smaller.<sup>3</sup> The limits are

<sup>2</sup> Since we consider flux rather than photon counts, the indices are shifted by 1 relative to Band (1993).

<sup>3</sup> It is interesting to note that  $|\alpha_2|$  is large for GRB 080319b, which might be an IC burst with a UV solution.

depicted in Fig. 3 for several values of the spectral indices. One can see that the available X-ray data rule out the UV solution for most of the phase space.

The IR solution holds for  $\nu_L < 0.1\nu_{\text{opt}} = 8 \times 10^{13}$  Hz and  $\alpha \leq -1.5$ . It requires a large electron Lorentz factor,  $\gamma_e \geq 1000$ , and a relatively low bulk Lorentz factor,  $\Gamma < 300$ . The solution is deep in the KN regime, and the KN suppression is very significant. It allows for a large amplification between the IR and the soft gamma-rays and no amplification between the low-energy gamma and the TeV emission. A solution is possible in a small region of the parameter space if the high-energy spectrum is steep ( $\alpha \leq -1.5$ ) – this increases the allowed flux at  $\nu_L$ . Such a spectrum above the peak frequency, though steeper than the canonical  $\alpha = -1.25$ , is not rare in the observations of prompt gamma-ray bursts.

To demonstrate the severity of the constraint, we plot (Fig. 4) the ‘allowed region’ in the  $(\gamma_e, \Gamma)$  phase space for which  $Y_H < 1$ . It is remarkable to note that the expected parameter region for internal shocks  $\gamma_e \approx 500$ ,  $\Gamma \approx 300$  is deep inside the ruled-out region. The parameter expected for external shocks  $\gamma_e \approx 50000$ ,  $\Gamma \approx 300$  is allowed with seed photon wavelength in the cm range. However, as we show in Section 4, self-absorption limits the amount of energy in such low-frequency seed photons, ruling out this solution. For low values of  $\gamma_e$ , the whole  $\Gamma$  range is seemingly allowed. However, this only happens at  $\gamma_e < 62, 34, 10$  for  $\alpha = 1.0, 0.5, 0$ , respectively, and therefore conflicts with the soft X-ray observations.

### 3 PAIR AVALANCHE

In cases when  $Y_H > 1$ , most of the electron energy is emitted as very high energy (TeV) gamma-rays. When the scattering is in the KN regime, that is, if equation (3) holds, the scattered photon has an energy of almost  $\gamma_e m_e c^2$  (in the fluid’s rest frame), and can therefore produce a pair when it encounters a typical low-energy gamma-ray photon with energy  $h\nu_\gamma/\Gamma$  (in this frame). More specifically, for a head-on collision between a photon with energy  $h\nu_\gamma = \xi\Gamma m_e c^2/\gamma_e$  and an electron with a Lorentz factor  $\gamma_e$ , the energies of the electron and the photon after the collision are

$$h\tilde{\nu} \approx \frac{4\xi}{1+4\xi} \Gamma \gamma_e m_e c^2 \quad (12)$$

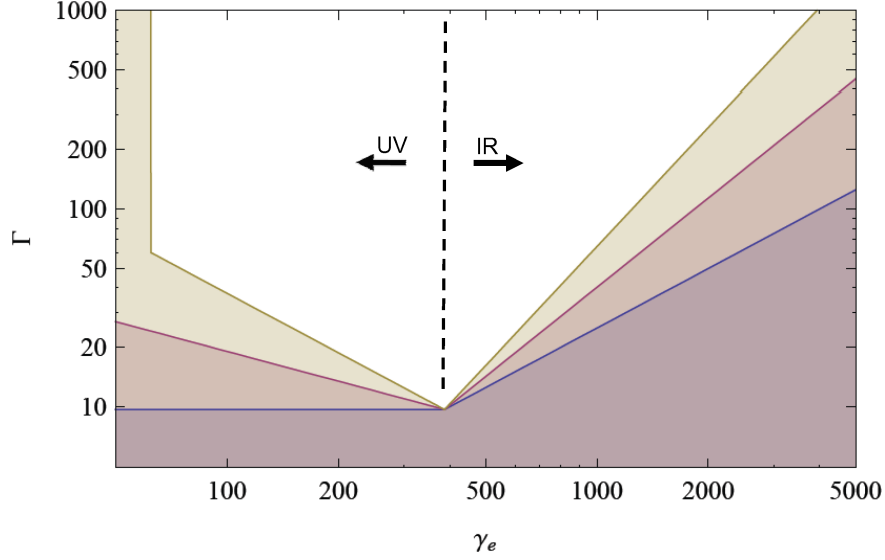


**Figure 4.** The allowed (coloured) phase space in which  $Y_H \leq 1$ . For three spectral indexes  $\alpha = 0, 0.5, 1$  (from bottom to top) for  $\nu_L > \nu_{\text{opt}}$  and  $\alpha = -1, -1.5, -2$  for  $\nu_L < \nu_{\text{opt}}$  (from bottom to top). Parameters used are as follows:  $F_\gamma/F_{\text{opt}} = 0.01$ ,  $\nu_{\text{opt}} = 8 \times 10^{14}$  Hz and  $h\nu_\gamma = 500$  keV. The  $\gamma_e$  axis corresponds to the values of  $\nu_L$  ranging from  $15\nu_{\text{opt}} = 4.8 \times 10^{16}$  Hz = 0.2 keV for  $\gamma_e = 50$  to  $0.006\nu_{\text{opt}} = 4.8 \times 10^{12}$  Hz for  $\gamma_e = 5000$ .

and

$$\hat{\gamma} \approx \frac{1}{1 + 4\xi} \gamma_e. \quad (13)$$

The resulting photon now has enough energy to collide with a photon with energy  $h\nu_\gamma$  and produce two electrons with Lorentz factor

$$\tilde{\gamma} \approx \frac{4\xi}{1 + 4\xi} \frac{\gamma_e}{2} \approx \frac{\gamma_e}{2}. \quad (14)$$

As the optical depth for pair creation is huge, all the scattered photons will create pairs with typical energy of  $\gamma_e m_e c^2 / 2$ . As a result we will have colder electrons and positrons with a ratio 2:1 in higher ( $\gamma_e/2$ ) and lower ( $\gamma_e/4\xi$ ) energies. These colder electrons and pairs will IC scatter more photons and will produce a second generation of cooler pairs with  $\gamma_e/4$ . The process will continue until pair creation stops. This will happen when  $\tilde{\gamma} h\nu_\gamma / \Gamma \approx m_e c^2$ . This situation was considered numerically by Coppi (1992), Stern et al. (1995) and Pe'er & Waxman (2005), and most recently by Vurm & Poutanen (2008).

If the physical conditions, like magnetic field and total number of particles, are fixed,  $\nu_L$ ,  $\nu_\gamma$  and  $\nu_H$  and the corresponding fluxes will vary as a result of the changing electron energy distribution due to the created pairs. These variations will be very significant because of the strong dependence (second and fourth powers) of the first two on  $\gamma_e$ . The dynamical evolution of such a system is interesting by itself. However, we are interested, here, in the final steady state in which  $\nu_\gamma$  and  $F_\gamma$  are fixed as the observed quantities. In this case, we can search for the physical parameters that exist in such a steady state. We can express  $\Gamma$  in terms of  $\gamma_e$  and  $\nu_\gamma$  using the pair creation threshold criteria (equation 3), and we can express  $\nu_L$  in terms of  $\nu_\gamma$  and  $\gamma_e$  (using equation 1). Given these expressions, we can estimate the steady-state  $Y_H$  as a function of  $\gamma_e$ .

Fig. 5 depicts the resulting  $Y_H$  values as a function of  $\gamma_e$  for different values of  $\alpha$ . The UV solution for  $\nu_L > 10\nu_{\text{opt}}$  and with rather low values of  $\gamma_e$  and  $\Gamma$  is possible. However, this solution suffers from the problems discussed earlier. It seems that if we impose the pair creation threshold conditions, the IR solution is ruled out with very high  $Y_H$  values (for any reasonable  $\alpha$ ). However,

as discussed earlier, there is a region in the parameter space for the IR solution for which  $Y_H \leq 1$ . In this case, only a small fraction of the energy goes into the high-energy photons, and it is possible (depending on time-scales) that most of the electrons cool down rapidly before pair avalanche arises.

#### 4 THE SEED PHOTONS AND SELF-ABSORPTION

A natural source of the seed photons is synchrotron emission by the same electrons that produce the IC emission. Assuming that this source is indeed synchrotron, we can proceed and estimate the strength of the magnetic field and the size of the emitting region. We can then check if these values are reasonable within given GRB models. However, we choose a more general approach and ask whether the large seed flux needed is limited by self-absorption.

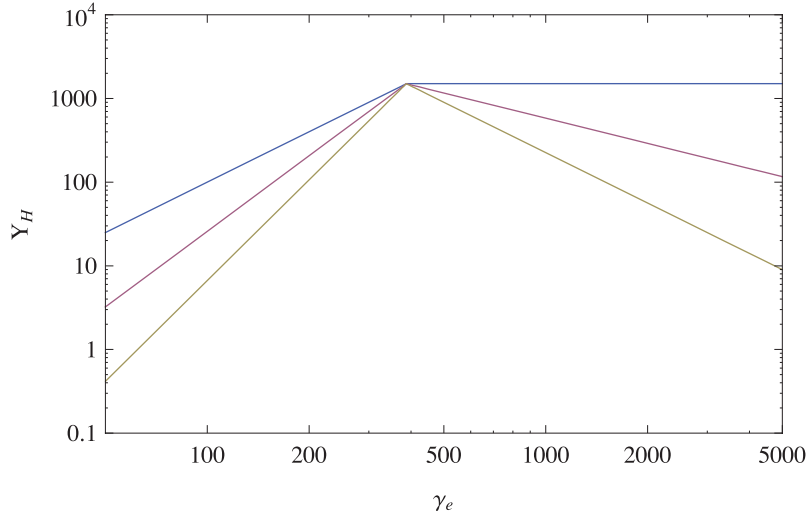
Self-absorption limits the flux at  $\nu_L$  to below the blackbody flux,  $F_{\text{sa}}$ , for a local temperature  $kT \approx \Gamma \gamma_e m_e c^2$ :

$$\begin{aligned} F_{\text{sa}}(\nu_L) &= \frac{2\nu_L^2}{c^2} \gamma_e m_e c^2 \frac{R^2}{4\Gamma d_L^2} \\ &\approx 1.3 \times 10^{-20} \text{ erg cm}^{-2} \text{ s}^{-1} \text{ Hz}^{-1} \\ &\times \frac{(R/10^{17} \text{ cm})^2}{d_L^2(z=1)} \frac{(\nu_\gamma/500)^2}{(\gamma_e/400)^3 (\Gamma/300)}, \end{aligned} \quad (15)$$

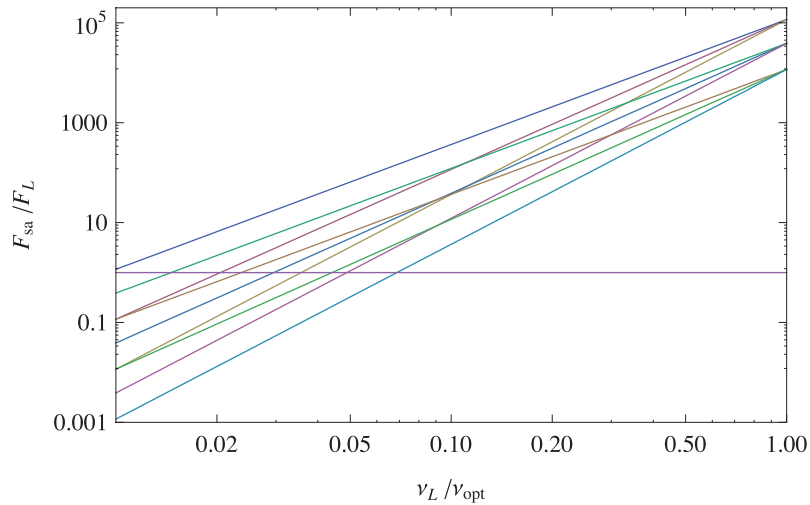
where  $R$  is the radius of the source and  $d_L(z=1)$  is the luminosity distance for  $z=1$ . In the following examples, we conservatively use  $R = 10^{17}$  cm as the emission radius of the prompt emission.

Fig. 6 depicts a comparison of this limiting flux,  $F_{\text{sa}}$ , with the needed flux  $F_L = F_\gamma \gamma_e^2 / Y_L$ . For  $\nu_L > 0.1\nu_{\text{opt}}$ ,  $F_{\text{sa}} < F_L$ . This implies that the electrons that produce the IC emission cannot produce the lower energy seed photons. The ratio  $F_{\text{sa}}/F_L$  decreases with increasing  $\Gamma$ . It also decreases when  $|\alpha|$  increases. So in most of the region where  $Y_H < 1$  (see Fig. 2), the seed flux is insufficient!

The combined limits on the  $(\Gamma, \gamma_e)$  parameter space from self-absorption with  $Y_H = 1$  are shown in Fig. 7. Only an extremely small region around  $\gamma_e \approx 1800$  (corresponding to  $\nu_L = 3.7 \times 10^{13}$  Hz) and  $\Gamma \approx 120$  is allowed. This used a conservative overestimate for



**Figure 5.** The steady-state  $Y_H$  as a function of  $\gamma_e$  for a situation in which pair avalanche leads to  $\gamma_e = m_e c^2 \Gamma / h\nu_\gamma$ . Shown are curves for three different values of  $\alpha = 0, 0.5, 1$  (from top to bottom) for  $\nu_L > \nu_{\text{opt}}$  and  $\alpha = -1, -1.5, -2$  for  $\nu_L < \nu_{\text{opt}}$ . The parameters used are as follows:  $F_\gamma / F_{\text{opt}} = 0.01$ ,  $\nu_{\text{opt}} = 8 \times 10^{14}$  Hz and  $h\nu_\gamma = 500$  keV. The  $\gamma_e$  axis corresponds to the values of  $\nu_L$  ranging from  $15\nu_{\text{opt}} = 4.8 \times 10^{16}$  Hz = 0.2 keV for  $\gamma_e = 50$  to  $0.006\nu_{\text{opt}} = 4.8 \times 10^{12}$  Hz for  $\gamma_e = 5000$ .



**Figure 6.** The ratio of the self-absorbed flux  $F_{\text{sa}}$  to the needed seed flux as a function of  $\nu_L / \nu_{\text{opt}}$  for three values of  $\Gamma = 100, 300, 1000$  (from top to bottom) and three different values of  $\alpha$ :  $\alpha = -1, -1.5, -2$  (from top to bottom) for  $\nu_L < \nu_{\text{opt}}$ . Parameters used in this figure are as follows:  $F_\gamma / F_{\text{opt}} = 0.01$ ,  $\nu_{\text{opt}} = 8 \times 10^{14}$  Hz and  $h\nu_\gamma = 500$  keV.

the emission radius  $R = 10^{17}$  cm. If we use the variability time-scale  $\delta t < 1$  s, with  $R \sim \Gamma^2 c \delta t$  and the low values of  $\Gamma$  obtained,  $R$  will be much smaller, invalidating even this solution. The self-absorption limit also rules out the region in the parameter space that corresponds to external shocks. This solution requires a very low seed frequency which would have implied a very small self-absorption limit.

## 5 CONCLUSIONS

For a typical GRB, IC has to amplify the total energy of a low-energy seed photon flux by a factor of  $\approx 1000$  to produce the observed prompt gamma-ray flux. The same relativistic electrons will, however, continue and upscatter the gamma-ray flux to very high energies in the TeV range. In many cases, this second-generation IC will be in the KN regime (i.e. the photon energy will be larger

than the electron's rest mass, in the electron's rest frame). This will somewhat suppress the efficiency of conversion of gamma-rays to very high energy gamma-rays, however it would not stop it altogether.

Our analysis focused on the case that the low-energy seed photons are produced within the moving region that includes the IC scattering relativistic electrons. Such will be the case, for example, in synchrotron self-Compton. Related considerations, which will be published elsewhere, apply when the seed photons are external and constrain IC processes in this case as well. The analysis is also limited to the important implicit assumption that the emitting region is homogenous. It is possible that very strong inhomogeneities could change this picture.

We have shown that, under quite general conservative assumptions, if IC produces the prompt MeV photons then a second scattering will overproduce a very high (GeV–TeV) prompt component

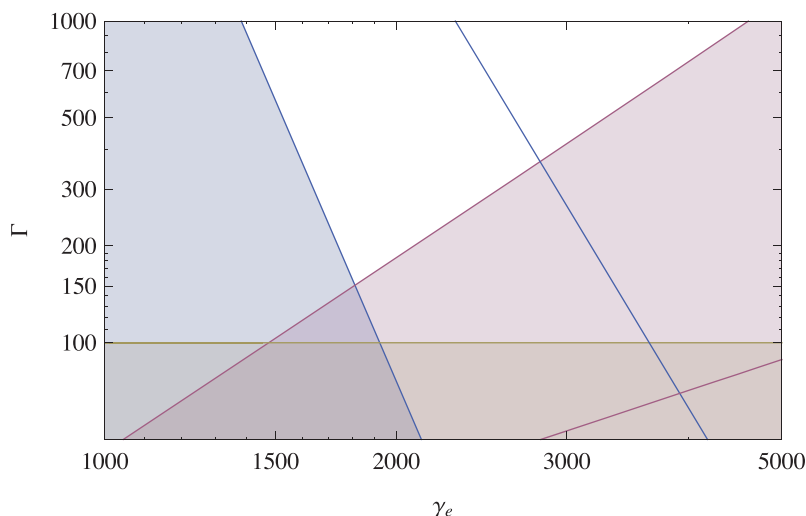


**Figure 7.** Allowed region for the IR solution in the  $(\Gamma, \gamma_e)$  parameter space. The limit on the left-hand side (decreasing curve) corresponds to the condition  $F_{\text{sa}} \geq F_L$ . The limit on the right-hand side (increasing curve) corresponds to  $Y_H = 1$ . Also marked is  $\Gamma = 100$ , which is considered as a minimal value for the bulk Lorentz factor to resolve the compactness problem (Lithwick & Sari 2001). The limits are shown for  $\alpha = -2$ . (On the right-hand side, around  $\gamma_e = 4000$  shown are the corresponding curves for  $\alpha = -1$ .) The  $\gamma_e$  range from 1000 to 5000 corresponds to  $\nu_L = 1.2 \times 10^{14}$  Hz to  $\nu_L = 4.8 \times 10^{12}$  Hz. Parameters used in this figure are as follows:  $F_\gamma/F_{\text{opt}} = 0.01$ ,  $\nu_{\text{opt}} = 8 \times 10^{14}$  Hz and  $h\nu_\gamma = 500$  keV. For  $\alpha = -2$ , an extremely small region around  $\gamma_e \approx 1800$  (corresponding to  $\nu_L = 3.7 \times 10^{13}$  Hz) and  $\Gamma \approx 120$  is allowed.

that will carry significantly more energy than the prompt gamma-rays themselves. On the theoretical front, such a component will cause an ‘energy crisis’ for most current progenitor models. From an observational point of view, this component is possibly already ruled out by EGRET upper limits (Gonzalez & Sanchez 2005; Ando et al. 2008). Fermi should very soon put much stronger limit to (or verify) this possibility. For example, a burst with isotropic energy  $E_{\gamma,\text{iso}} = 10^{53}$  erg, located at  $z = 1$ , would produce  $\sim 100 Y_H (E_H/10 \text{ GeV})$  photons detected by Fermi.

One may not overproduce a high-energy component if the seed photons are in the UV regime. However, in this case, the needed seed photon energy should be equal to or larger than the observed prompt gamma-ray energy. Downwards extrapolation of the X-ray observations put strong limits on this solution, and probably rules it out as well. Moreover, this UV solution requires pair loading to be efficient.

## ACKNOWLEDGMENTS

We thank R. Mochkovitch, E. Nakar, J. Poutanen, P. Kumar and X. F. Wu for helpful discussions. The research was partially supported by the ISF center for excellence in High Energy Astrophysics, by an Israel–France collaboration grant, by an IRG grant, by an ATP grant and by the Schwartzman chair.

## REFERENCES

- Akerlof C. et al., 1999, *Nat*, 398, 400  
 Ando S., Nakar E., Sari R., 2008, *ApJ*, 689, 1150  
 Band D. et al., 1993, *ApJ*, 413, 281

- Bloom J. S. et al., 2008, *ApJ*, in press (arXiv:0803.3215)  
 Cohen E., Katz J. I., Piran T., Sari R., Preece R. D., Band D. L., 1997, *ApJ*, 488, 330  
 Coppi P. S., 1992, *MNRAS*, 258, 657  
 D’Elia V. et al., 2008, *ApJL*, submitted (arXiv:0804.2141)  
 Fan Y. Z., Piran T., 2008, *Front. Phys. China*, 3, 306  
 Ghisellini G., Lazzati D., Celotti A., Rees M. J., 2000, *MNRAS*, 316, L45  
 Gonzalez Sanchez M. M., 2005, PhD thesis  
 Kobayashi S., Zhang B., Mészáros P., Burrows D., 2007, *ApJ*, 655, 391  
 Kumar P., McMahon E., 2008, *MNRAS*, 384, 33  
 Kumar P., Panaitescu A., 2008, *MNRAS*, 391, L19  
 Lithwick Y., Sari R., 2001, *ApJ*, 555, 540  
 Pe’er A., Waxman E., 2005, *ApJ*, 628, 857  
 Preece R. D., Briggs M. S., Malozzi R. S., Pendleton G. N., Paciesas W. S., Band D. L., 1998, *ApJ*, 506, L23  
 Preece R. D., Briggs M. S., Giblin T. W., Malozzi R. S., Pendleton G. N., Paciesas W. S., Band D. L., 2002, *ApJ*, 581, 1248  
 Racusin J. L. et al., 2008, *Nat*, 455, 183  
 Sari R., Piran T., 1997, *MNRAS*, 287, 110  
 Sari R., Narayan R., Piran T., 1996, *ApJ*, 473, 204  
 Shaviv Nir J., Dar A., 1995, *MNRAS*, 277, 287  
 Shemi A., 1994, *MNRAS*, 269, 1112  
 Stern B. E., Poutanen J., 2004, *MNRAS*, 352, L35  
 Stern B. E., Begelman M. C., Sikora M., Svensson R., 1995, *MNRAS*, 272, 291  
 Vurm I., Poutanen J., 2008, *ApJ*, submitted (arXiv:0807.2540)  
 Waxman E., 1997, *ApJ*, 485, L5  
 Yost S. A. et al., 2007, *ApJ*, 669, 1107  
 Yu Y. W., Wang X. Y., Dai Z. G., 2008, *ApJ*, in press (arXiv:0806.2010)  
 Zou Y. C., Piran T., Sari R., 2008, *ApJ*, in press (arXiv:0812.0318)

This paper has been typeset from a  $\text{\TeX}/\text{\LaTeX}$  file prepared by the author.